Measurement of the ^{115}In (γ,γ^{′})^{115m}In inelastic scattering cross section in the 1.8 to 3.7 MeV energy range with monoenergetic photon beams

W. Tornow, M. Bhike, S. W. Finch, Krishichayan, and A. P. Tonchev

Phys. Rev. C **98**, 064305 — Published 6 December 2018

DOI: 10.1103/PhysRevC.98.064305

Measurement of the ^{115}In$(\gamma,\gamma')^{115m}$In inelastic scattering cross section in the 1.8 to 3.7 MeV energy range with mono-energetic photon beams

W. Tornow,* M. Bhike, S.W. Finch, and Krishichayan
Department of Physics, Duke University, Durham, North Carolina 27708, USA
and Triangle Universities Nuclear Laboratory, Durham, North Carolina 27708, USA

A.P. Tonchev
Nuclear and Chemical Sciences Division, Lawrence Livermore National Laboratory, Livermore, California 94550, USA
(Dated: October 8, 2018)

For the first time the excitation cross section of ^{115}In to its first excited state at 336.24 keV has been measured with mono-energetic photon beams at 15 energies between 1.8 and 3.7 MeV. The measurements were performed at the HIγS facility with natural In targets and incident photon fluxes ranging from $0.7 \times 10^7 \gamma/(\mathrm{cm}^2 s)$ to $3.2 \times 10^7 \gamma/(\mathrm{cm}^2 s)$. The inelastic scattering cross section was obtained from the yield of the 336.24 keV de-excitation γ rays. The cross-section values varied between < 0.05 μb and 28.7 μb at 1.8 MeV and 3.7 MeV, respectively. Compared to standard photon inelastic scattering cross-section data in this energy range of medium-mass nuclei, these extremely small values are not completely unexpected, given the nature of the low-lying nuclear levels of ^{115}In. Model calculations, however, overestimate the measured cross-section data by approximately one order of magnitude. Using different choices for the E1 γ-ray strength function, the data can be well described. The data are important for improving our knowledge of the level scheme of ^{115}In, especially spin and parity assignments of already known states.

I. INTRODUCTION

In 1938 Goldhaber, Hill, and Szilard [1] reported the excitation of an excited state of ^{115}In and provided the first conclusive evidence for nuclear isomerism in a stable nucleus. They observed that the 4.1 h activity could be produced by fast neutrons from a Rn-Be source, but not by slow neutrons. The measured activity was attributed to a new type of nuclear process: a nuclear excitation leading to a metastable state in ^{115}In. Almost at the same time, the first photoexcitation of the ^{115}In isomer was performed by Pontecorvo and Lazard [2] by irradiating natural indium foils with a 1.73-MeV endpoint-energy bremsstrahlung beam. They showed that photoexcitation is an alternative method to neutron irradiation and confirmed the hypothesis of nuclear isomerism. Following these early experiments, the ^{115m}In isomer became the subject of many studies investigating the probability of populating this isomeric state using different probes and different incident energies [3–7].

The main reason for the existence of the ^{115}In isomer is the large difference between the isomeric and the ground state spins of $\Delta J = 4$, resulting in a greatly reduced transition probability between these two states. Therefore, the ^{115m}In isomer belongs to the category of the so-called spin isomers [8]. It also belongs to the group of $g_{9/2}$ isomers, referring to the mass region of nuclei with protons or neutrons numbers just less than that of the filled $N = 50$ shell. It is also interesting to note that the spins and parities for these $g_{9/2}$ isomers are "inverted" with respect to their ground states, i.e., the ground state has the higher spin of $J^\pi = 9/2^+$, while the isomeric state has the lower spin of $J^\pi = 1/2^-$. Located at 336.244 keV excitation energy, it decays 95% of the time to the ground state of ^{115}In with $T_{1/2}$ =4.486 h and γ-ray intensity of $I_\gamma = 45.9\%$. The remaining 5% β decays to ^{115}Sn, as does the unstable ground state of ^{115}In ($T_{1/2} = 4.41 \times 10^{14}$y [9]).

The excitation energy range of ^{115}In up to 1.8 MeV contains only three known states with definite J^π values and four known states with tentative assigned J^π values which could be populated from the ground state via dipole excitation by incident real photons with energies below 1.8 MeV [9]. Subsequently, these excited states could cascade down to the isomeric 1st excited state. These states are often referred to as intermediate states (IS) or doorway states, because they allow population of the isomeric excited state from the ground state. Considering also quadrupole transitions, the picture does not change much. In this case an additional three states of definite J^π assignments and two of tentative J^π assignments could act as IS. Because of the small number of possible IS, only a relatively small probability exits for exciting ^{115m}In with incident photons below 1.8 MeV.

Although the ^{115}In level scheme is rather poorly known above 2.5 MeV excitation energy with 20 levels of unknown J^π below 4 MeV, there are up to 20 potential states which could be excited by 1.8 to 4 MeV incident dipole photons, and which could subsequently cascade down to the 1st excited state (see Fig. 1). The situation may be more favorable if E2 excitations are considered as well, although their strength is much smaller than E1 or M1 excitations. In this case an additional six known states with tentatively assigned J^π values could serve as IS in the 1.8 to 4 MeV incident photon energy range.

In the past, the ^{115}In$(\gamma,\gamma')^{115m}$In reaction has

* tornow@tunl.duke.edu

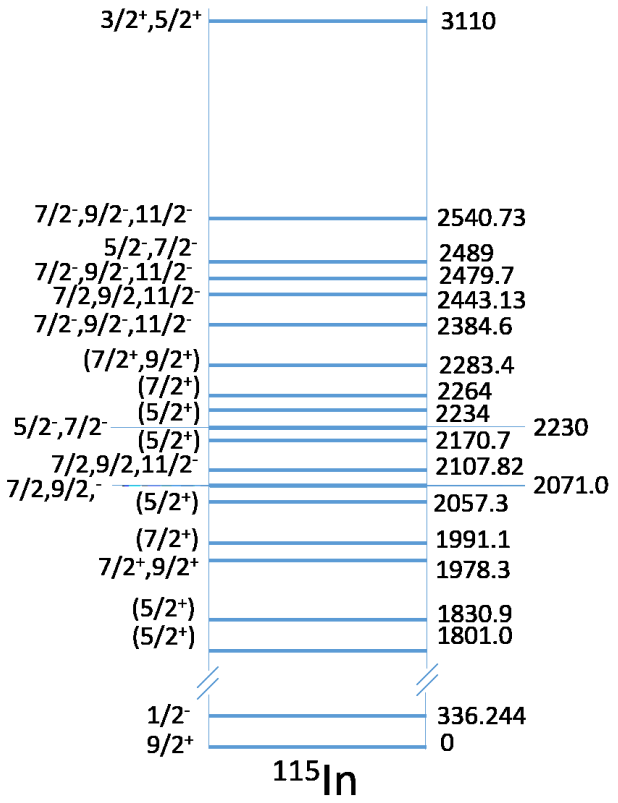

FIG. 1. (Color online) Partial level scheme of ^{115}In [9]. The present status of the spin and parities are shown on the left side of the partial level scheme, while corresponding energies in keV are shown on the right side. The energy separation between the ground state and the isomeric state at 336.24 keV is not to scale.

been studied in the energy range considered in the present work with radioactive sources [10, 11] and with bremsstrahlung photon beams with endpoint energies as low as approximately 1 MeV. The most recent studies with bremsstrahlung photons were performed by von Neumann-Cosel *et al.* [12] using the S-DALINAC electron accelerator at Darmstadt and by Belic *et al.* [13] using the DYNAMITRON accelerator at Stuttgart. The work of Ref. [12] involved photon beams with 13 endpoint energies between 2.0 and 4.5 MeV. Based on kinks in the excitation function of the measured 336.24 keV yield, it was found that significant strength is located in the excitation energy range between 2.7 and 2.9 MeV, and between 3.2 and 3.4 MeV. The currently known level scheme of ^{115}In does not show any states which could serve as IS in these two energy intervals. The work of Ref. [13] discovered four IS in ^{115}In below 1.7 MeV, and three IS at excitation energies of 1980, 2420 and 2950 keV with energy uncertainties of the order of 30 keV. It is interesting to point out that the IS reported in Ref. [13] at 940 keV coincides with the excited states in ^{115}In located at 934 keV with $J^\pi = 7/2^+$, and at 941 keV with $J^\pi = 5/2^+$, the latter indicating that E2 excitations could play a role. Quadrupole excitations have also been identified in nuclear resonance fluorescence measurements on ^{115}In [12–18].

Earlier photoexcitation work performed by Booth and Brownson [19] which led to the identification of IS below 2 MeV excitation energy is in general consistent with the findings of Ref. [13]. Concentrating on the 1.8 to 4 MeV energy region of interest in the present study, we note that the results of Refs. [12] and [13] do not provide a consistent picture, except maybe for the IS at 2950 keV reported in Ref. [13], which is just outside of the 2.7 to 2.9 MeV energy range referred to in Ref. [12].

Given the inherent limitations associated with bremsstrahlung beams, as also documented by the results obtained in Refs. [12] and [13], the use of mono-energetic photon beams, although less intense, may result in more accurate and complete determinations of the IS structure of ^{115}In for excitation energies above 1.8 MeV. This conjecture is one of the justifications for the experimental studies described below. Another reason for studying the ^{115}In$(\gamma,\gamma')^{115m}$In reaction is related to its potential use as convenient photon flux monitor at low energies, where suitable monitors are missing.

II. EXPERIMENTAL APPROACH

Mono-energetic photon beams were produced at the High-Intensity Gamma-ray Source (HIγS) of the Triangle Universities Nuclear Laboratory (TUNL) at 15 energies in the 1.8 MeV to 3.7 MeV energy range. Free-electron laser infrared photons with wavelength of 1070 nm were backscattered of relativistic electrons circulating in a 1.2 GeV electron storage ring with currents between 60 mA and 90 mA. The electron energy was adjusted between 384 MeV and 455 MeV and the current in the wiggler electro-magnets was changed to provide the photon beam energies of interest. After passing through a pre-collimator the photon beam entered a collimator hut where its diameter was reduced via a 6" long collimator made of lead to either 0.75" or 1" depending on the time the experiments were performed. Most of the cross-section data reported here for the ^{115}In$(\gamma,\gamma')^{115m}$In reaction were measured concurrently with data obtained for the ^{180m}Ta$(\gamma,\gamma')^{180}$Ta reaction during the years 2015 to 2017. A typical photon energy spectrum is shown in Fig. 2. It was measured with a 123% efficient (relative to a 3" $\times$ 3" NaI detector) HPGe detector placed at 0° degrees relative to the photon beam direction. It was obtained from the comparison of a Monte-Carlo simulation of the HPGe detector pulse-height spectrum to the measured pulse-height spectrum. The tail seen in Fig. 2 below 2400 keV is an artifact caused by low statistics and our deconvolution procedure. Due to heavy use in beam, this HPGe detector has developed a low-energy tail in its pulse-height response. This effect can be seen with γ-ray test sources and is not currently incorporated

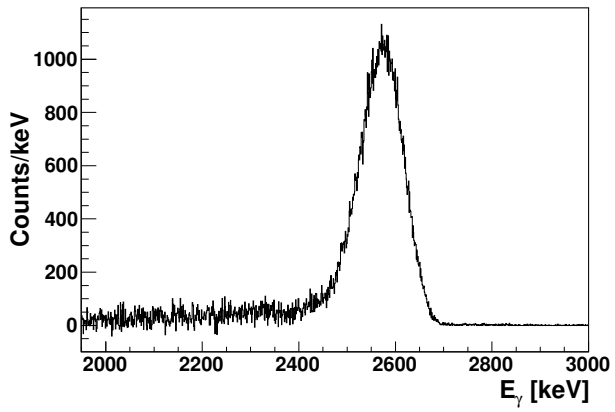

FIG. 2. Photon energy spectrum at $E_\gamma = 2.59$ MeV obtained from a HPGe detector pulse-height spectrum, as described in the text.

in the Monte-Carlo simulation based conversion of our measured pulse-height spectrum into the photon energy spectrum of Fig. 2. Following kinematics, the photon flux approaches zero at approximately 2250 keV. For such photon energy measurements the incident photon flux had to be reduced to less than 20 kHz. This was accomplished by inserting copper attenuators in the photon beam path ≈ 40 m upstream of the HPGe detector. As can be seen from Fig. 2, the FWHM of the photon beam energy distribution is 100 keV with centroid energy of 2.59 MeV. The photon energy spectrum is slightly asymmetric, as expected from the slight divergence of the interacting electron and FEL photon beams, and the finite collimator size. The full width is approximately twice as large as the FWHM. The uncertainty in the energy calibration of the HPGe detector is less than ± 0.2 keV below 3 MeV and less than 0.3 keV above this energy. The uncertainty of the measured centroid photon energy is typically 5 keV or less.

The incident photon flux was obtained from auxiliary measurements performed with an 8" diameter and 12" long NaI detector with efficiency of 99%. This detector was rotated into the beam with copper attenuators placed in the beam path as was done for the measurements with the HPGe detector referred to above. The yield recorded with a 1 mm (in some cases 0.5 mm) thin plastic scintillator paddle placed in the beam path after the collimator (see Fig. 3 for a schematic of the experimental setup) was normalized to the NaI detector yield. For the actual $^{115}\mathrm{In}(\gamma,\gamma')^{115m}\mathrm{In}$ activation measurements the NaI and the HPGe detector were rotated out of the photon beam direction, and the rate recorded with the calibrated plastic scintillator paddle provided a measure of the incident photon flux. The scintillator paddle was calibrated relative to the NaI detector at each photon energy. The copper attenuators referred to above were also used to measure the count-rate response of the scintillator paddle over a five order of magnitude varying

TABLE I. Photon energy E_γ with associated energy spread (FWHM), photon flux Φ_γ, and $^{115}\mathrm{In}(\gamma,\gamma')^{115m}\mathrm{In}$ cross-section data obtained in the present work.

E_γ [MeV]	Φ_γ [cm^{-2}s^{-1}]	σ [μb]
1.80 ± 0.03	$(7.05 \pm 1.06) \times 10^6$	< 0.05
1.90 ± 0.03	$(4.97 \pm 0.75) \times 10^6$	0.37 ± 0.09
2.00 ± 0.04	$(6.07 \pm 0.91) \times 10^6$	0.47 ± 0.10
2.10 ± 0.04	$(4.99 \pm 0.75) \times 10^6$	1.88 ± 0.34
2.20 ± 0.04	$(5.68 \pm 0.85) \times 10^6$	< 0.09
2.30 ± 0.04	$(5.67 \pm 0.85) \times 10^6$	2.10 ± 0.37
2.40 ± 0.05	$(9.63 \pm 1.44) \times 10^6$	1.87 ± 0.30
2.50 ± 0.05	$(1.35 \pm 0.20) \times 10^7$	5.86 ± 0.94
2.59 ± 0.05	$(1.21 \pm 0.18) \times 10^7$	4.39 ± 0.89
2.80 ± 0.06	$(2.57 \pm 0.51) \times 10^7$	5.64 ± 1.15
2.95 ± 0.06	$(1.62 \pm 0.32) \times 10^7$	18.7 ± 3.8
3.12 ± 0.06	$(2.68 \pm 0.54) \times 10^7$	13.2 ± 2.7
3.30 ± 0.07	$(1.96 \pm 0.39) \times 10^7$	6.75 ± 1.38
3.60 ± 0.07	$(3.22 \pm 0.64) \times 10^7$	23.5 ± 4.8
3.70 ± 0.07	$(2.70 \pm 0.54) \times 10^7$	28.7 ± 5.8

incident photon flux. Excellent linearity was found with incident photon fluxes up of $5 \times 10^7\ s^{-1}$, corresponding to approximately 5×10^5 pulses s^{-1}. The second column of Table I gives the photon fluxes for the cross-section data obtained in the present work. In general, the photon flux increases with energy and then drops off at the highest energy. As stated already, the data were taken during the years 2015 to 2017 in six individual run cycles. The variation in mirror conditions and maximum electron current used are responsible for the fluctuations of the photon flux from the general trend referred to above.

The NaI pulse-height spectrum was also carefully investigated and recorded at different PMT high-voltage settings to check on any bremsstrahlung contributions in the beam, which potentially could falsify our cross-section measurements. The HPGe detector spectra were also used for this purpose. No measurable amounts of bremsstrahlung contributions were detected in these tests. In addition, at a photon energy of 1.8 MeV activation measurements were performed using foils of Au and Ni with (γ, n) thresholds ranging between 8.077 MeV (^{197}Au) and 12.218 MeV (^{58}Ni). After irradiation, these foils were γ-ray counted using the same HPGe detector as used for the ^{115m}In counting. No activity was found above background, clearly showing that bremsstrahlung contributions with energies above the (γ, n) threshold had to be at least five orders of magnitude lower than the 1.8 MeV photons of interest. Therefore, even if the effective $^{115}\mathrm{In}(\gamma,\gamma')^{115m}\mathrm{In}$ cross section is a factor of 100 larger for bremsstrahlung photons, its effect on the present data is at least one order of magnitude lower than the uncertainty assigned to the photon flux determination

The natural In targets used in the present experiment consisted of 1" diameter disks with total mass of approximately 2 g. Typically, they were irradiated for 20 hours

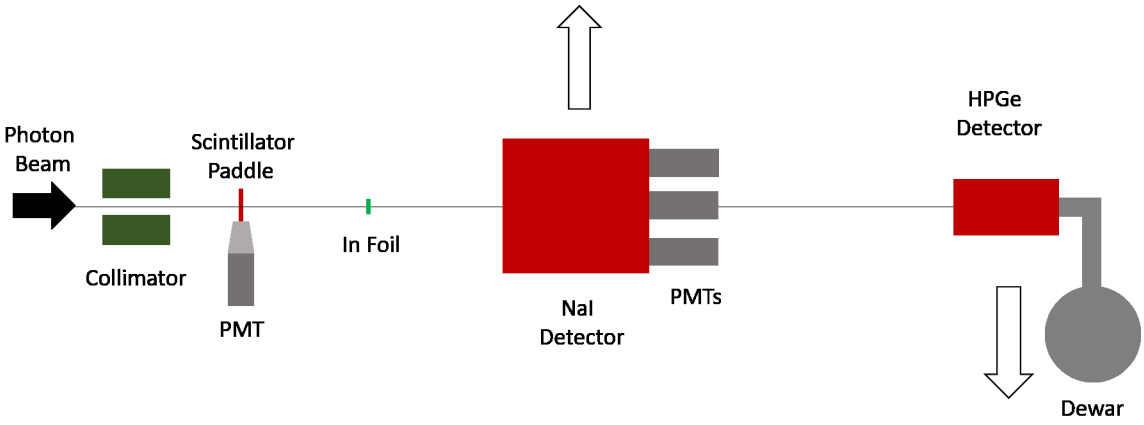

FIG. 3. (Color online) Schematic diagram (not to scale) of the experimental setup consisting of photon beam collimator, scintillator paddle, and In activation foil. The NaI detector of known efficiency is used for cross-calibrating the scintillator paddle rate. The HPGe detector is used for photon beam energy measurements. Both detectors are rotated out of the photon beam during the activation measurements.

at each energy. This time is longer than necessary, but the longer exposure time was dictated by the Ta foils irradiated concurrently.

After irradiation, the In foils were γ-ray counted with a Canberra HPGe detector and standard data-acquisition hardware and software. The foils were placed on a plastic cap mounted on the front face of the detector. The efficiency of the detector for this special counting configuration was determined experimentally by measuring the efficiency with calibrated γ-ray point sources at different radial distances r from the center position. Integration over this r dependent efficiency from the center to the maximum radius of the In disks provided the efficiency $\epsilon = 0.26 \pm 0.01$ needed for converting the measured 336.24 keV γ-ray yield to absolute cross-section values, using the γ-ray flux values of Table I, and the γ-ray intensity $I_\gamma = 0.459 \pm 0.020$. The γ-ray attenuation through the In foil was corrected for by using the attenuation data for In available at NIST [20].

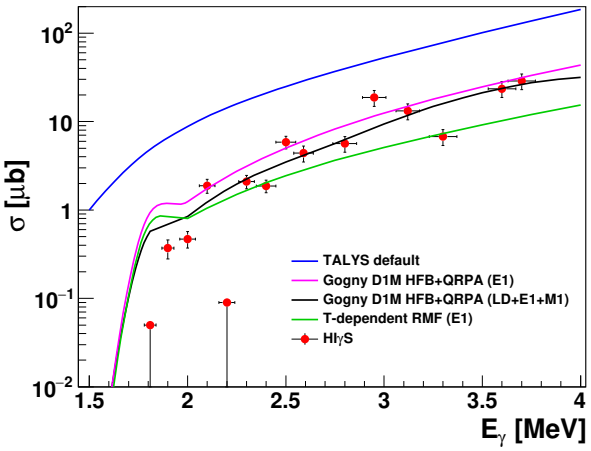

FIG. 4. (Color online) Measured cross-section data for the reaction ^{115}In$(\gamma,\gamma')^{115m}$In in comparison to different TALYS-1.9 [21, 22] evaluations. The model parameters are detailed in the text.

III. RESULTS

Our results for the ^{115}In$(\gamma,\gamma')^{115m}$In cross section are tabulated in Table I and plotted in Fig. 4. As can be seen, the cross-section values increase from < 0.05 μb at 1.8 MeV to 28.7 μb at 3.7 MeV, with the data at 1.8 MeV and 2.2 MeV not following this general trend. At these two incident photon energies no counts above background were observed at 336.24 keV. Therefore, the quoted cross-section values present only an upper limit.

The overall uncertainty of our data is governed by the uncertainty associated with the photon flux determination. As stated earlier, a scintillator paddle was used, which was calibrated relative to a 99% efficient NaI detector at a low photon flux compared to the ones used during the actual activation runs. Although this cross calibration was done at each energy, the count-rate linearity of the scintillator paddle was assumed to not have changed during the course of the measurements. It was assumed that the gain of the photo-multiplier tube remained constant from one measurement to the other. In order to account for possible variations, a conservative 15% uncertainty was assigned to the photon flux determinations for fluxes up to 1.5×10^7 photons/(cm^{2}s). This estimate was increased to 20% for photon fluxes above this value. The statistical uncertainty associated with the 336.24 keV γ-ray yield varied between 0.8% and 16.7%. The uncertainty of the γ-ray intensity I_γ is 0.2% [9]. The uncertainty of the γ-ray absorption in the foils is 3% [20]. The efficiency of the HPGe detector is known to 4.5%. The individual uncertainties were added in quadra-

ture and the resulting overall cross-section uncertainty is quoted in Table I, ranging from 16% to 23%, except at 1.8 and 2.2 MeV, where the assigned uncertainty is 0.02 μb and 0.05 μb, respectively.

The small upper limit for the cross-section ($<$ 0.05 μb) found at 1.8 MeV is consistent with the known level scheme of ^{115}In (see Fig. 1). Given the 60 keV FWHM and approximately full width of 120 keV, there are only the two states located at 1801.0 keV and 1830.9 keV with tentative $J^\pi = (5/2^+)$ that could provide suitable IS, but only via electric quadrupole E2 transitions from the $9/2^+$ ground state with small probability.

Similar arguments hold for the small upper limit for the cross section ($<$ 0.09 μb) found at 2.2 MeV, where the two states located at 2170.7 keV and 2234.0 keV with tentative $J^\pi = (5/2^+)$ could act as IS, but again only via E2 transitions from the ground state, while the state at 2264 keV with tentative $J^\pi = (7/2^+)$ does not have sufficient overlap with the associated incident photon energy distribution. In addition, the required magnetic dipole M1 radiation character provides only a small transition probability from the ground state. The state at 2230 keV has a J^π assignment of either $5/2^-$ or $7/2^-$. The small cross section determined in the present work rules out the $7/2^-$ assignment (electric dipole E1 transition from the ground state) in favor of the $5/2^-$ assignment (magnetic quadrupole M2 radiation with extremely small probability).

Moving on to the 1.9 MeV datum, we note that the current level scheme of ^{115}In does not contain any levels which could serve as IS for this incident photon energy. Because the 336.24 keV transition has been observed in the present work, we conclude that there must exist at least one suitable state in the excitation energy range between 1850 keV and 1950 keV.

For E_γ = 2.0 MeV there exists almost perfect overlap with the 1991.1 keV state which could be excited via M1 photons from the ground state if the tentative $J^\pi = (7/2^+)$ is correct. The state at 1978.3 keV with either $J^\pi = 7/2^+$ or $9/2^+$ will also contribute via M1 radiation. In addition to this state, the 2057.3 keV state with tentative $J^\pi = (5/2^+)$ could contribute slightly to the observed strength via an E2 transition from the ground state.

The cross-section value observed at 2.1 MeV incident photon energy is about a factor of four larger than that found at 2.0 MeV. This fact can easily be explained by considering the known states involved. First, the state located at 2057.3 keV with tentative $J^\pi = (5/2^+)$ already referred to above is a candidate. Second, the state at 2071.0 keV with either $J = 7/2$ and unknown parity, requiring E1 or M1 radiation, or $J^\pi = 9/2^-$ requiring E1 radiation could also act as IS. Third, and even more important, the state at 2107.82 keV with spin of either $J = 7/2$ or 9/2, but unknown parity, requiring again either E1 or M1 radiation, or $J^\pi = 11/2^-$ with E1 radiation from the ground state are potential IS. The state at 2170.7 keV with tentative $J^\pi = (5/2^+)$ has insufficient overlap with the incident photon beam energy distribution.

The cross-section datum measured in the present work at 2.3 MeV may include the contribution of an M1 transition from the ground state to the state located at 2283.4 keV with tentative $J^\pi = (7/2^+)$ or $(9/2^+)$. The state at 2264 keV with tentative $J^\pi = (7/2^+)$ may contribute as well, although to a smaller degree, while the state at 2234.0 keV with tentative $J^\pi = (5/2^+)$ can almost be ignored due to its very small energy overlap and required E2 transition character.

The states located at 2384.6 keV and 2443.13 keV are of interest at E_γ = 2.4 MeV. The former is accessible from the ground state via E1 radiation. Similarly, if the state at 2443.13 keV has $J^\pi = 7/2$ or 9/2 with unknown parity, it could be excited by E1 or M1 radiation. Furthermore, if this state has $J^\pi = 11/2^-$, it could serve as IS for an E1 transition from the ground state. As a result, the available level scheme of ^{115}In could predict a sizable cross section. The two states located at 2479.7 keV and 2489 keV are not expected to contribute due to their lack of energy overlap with the incident photon beam with centroid energy of E_γ = 2.4 MeV.

However, the two states referred to in the last sentence are of importance at E_γ = 2.5 MeV. Again, if the J^π values are $7/2^-$, $9/2^-$, or $11/2^-$ the state at 2479.7 keV could be reached via E1 radiation from the ground state. The same is true for the 2489 keV state if its J^π value is $7/2^-$ and not $5/2^-$(the latter requiring an M2 transition). Finally, the state at 2540.73 keV could serve as IS for E1 radiation.

The state at 2540.73 keV may also contribute to the cross section measured at E_γ = 2.59 MeV.

The current level scheme of ^{115}In does not provide any information to support or explain the cross-section values observed at 2.8 MeV and 2.95 MeV.

The cross section observed at 3.1 MeV may be partially caused by the 3110 keV state with tentative $J^\pi = (5/2^+)$ assignment requiring an E2 transition from the ground state. Information is not available to discuss the cross-section values observed in the present work for incident photon energies above 3.3 MeV.

Comparing our results to the previous work with bremsstrahlung beams we note that the IS location identified in the 2.7 to 2.9 MeV photon energy range by von Neumann-Cosel *et al.* [12] is consistent with our finding at 2.8 MeV and especially at 2.95 MeV. However, our data do not confirm a strong IS centered at 3.3 MeV and observed in Ref. [12]. The locations of the IS found by Belic *et al.* [13] at 1980 keV and 2420 keV are in agreement with our work. In addition, our data confirm the IS found in Ref. [13] at 2950 keV. Considering the uncertainties of the data, the ratio of the observed strength is also consistent with the present work.

Figure 4 shows our data in comparison to a TALYS [21] calculation using the default values of this statistical model computer code (blue curve). The TALYS prediction is a factor of ≈ 7 higher than our experimental data.

In order to gain some insight, the different level density parameterizations available in TALYS were used to calculate the ^{115}In$(\gamma,\gamma')^{115m}$In cross section. The default level density is the constant temperature plus Fermi gas model [23]. Additional level density models include the back-shifted Fermi gas model [24], the generalized superfluid model [25], and three microscopic level densities based on the Skyrme force from either Goriely's or Hilaire's tables, and the temperature dependent Hartree-Fock-Bogoliubov plus Gogny force from Hilaire's combinatorial tables [26]. Surprisingly, the calculated cross section shows hardly any sensitivity for photon energies below 3 MeV. Above this energy, the back-shifted Fermi gas model provides the largest cross section, while the microscopic level density with the Gogny force predicts the smallest cross section.

Next, we studied the effect of the E1 γ-ray strength function. The default TALYS cross sections are based on the Brink-Axel Lorentzian parameterization [27, 28]. There are an additional six E1 γ-ray strength functions available in TALYS, all of them giving considerably smaller cross-section values. Figure 4 shows cross-section curves for the E1 strength function with the highest (Gogny DIM HFB+QRPA) [29, 30] and lowest (T-dependent RMF) predicted cross section. As can be seen, they are in much better agreement with the experimental data than the calculations performed with the default Brink-Axel Lorentzian.

We also investigated the role of the M1 γ-ray strength function. By default, TALYS normalizes the M1 strength function to the E1 strength function as $f_{E1}/(0.0588A^{0.878})$. When using the other available M1 strength function in TALYS, the calculated cross section hardly changed, indicating that the M1 γ-ray strength function has less of an influence on the cross section of interest than the E1 γ-ray strength function. TALYS-1.9 also provides the new option Gogny-DIM HFB+QRPA [30] for M1 strength. For consistency we used the Gogny-DIM HFB+QRPA strength function for both E1 and M1, and the microscopic level density including Gogny force. The calculated ^{115}In$(\gamma,\gamma')^{115m}$In cross section using these model parameters (black curve in Fig. 4) is in very good agreement with our experimental data.

Of course, the question remains whether or not the modification of the γ-ray strength function models and parameterizations discussed above is just a convenient way of compensating for the poorly known and apparently non-statistical nature of the level scheme of ^{115}In in the excitation energy range of the present experimental work. We also calculated the ^{115}In$(\gamma,n)^{114}$In cross section up to 25 MeV using the same Gogny-DIM HFP+QRPA E1 and M1 strength functions as well as the level density including the Gogny force. This calculated cross section is in good agreement with the evaluated cross section of Varlamov *et al.* [31], as can be seen in Fig. 5. For comparison, Fig. 5 also gives the ^{115}In$(\gamma,n)^{114}$In cross section as calculated by TALYS using its default values, indicating that different choices

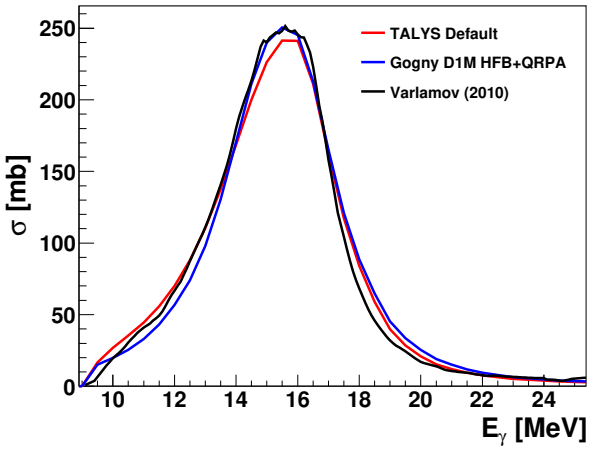

FIG. 5. (Color online) The ^{115}In$(\gamma,n)^{114}$In cross section up to 25 MeV. The evaluated cross section of Varlamov *et al.* [31] (black curve) is compared to TALYS-1.9 using the default values (red curve) and using the Gogny D1M HFB+QRPA model for the level density, E1, and M1 strength.

for the γ-ray strength functions have only a minor effect on the (γ,n) cross section, as expected. Therefore, ^{115}In$(\gamma,\gamma')^{115m}$In cross-section data in the 4 MeV $< E <$ 20 MeV energy range are needed to better determine the γ-ray strength functions.

IV. SUMMARY AND CONCLUSIONS

The cross section of the ^{115}In$(\gamma,\gamma')^{115m}$In reaction was measured for the first time with mono-energetic photon beams at 15 energies in the 1.8 to 3.7 MeV energy range and found to vary between less than 0.05 μb and 28.7 μb. These are the smallest cross-section values measured at HIγS with low-energy photon beams. The data provide a new basis for a convenient off-line low-energy photon flux monitor needed for activation experiments at low photon energies. The location of most of the kinks in the excitation function of the ^{115}In$(\gamma,\gamma')^{115m}$In reaction observed in Refs. [12, 13] with bremsstrahlung beams and interpreted as intermediate states or doorway states are confirmed by the present measurements. This finding demonstrates the power of monoenergetic photon beams in determining the spin and parity of states located in the quasi-continuum and linked to the isomeric state of interest. Our cross-section data are ≈ 7 times lower than predicted by the TALYS statistical model using its default input parameters. E1 γ-ray strength function models other than the default Brink-Axel Lorentzian parameterization provide considerably smaller cross-section values, in good agreement with our data. The present data could be used to improve the current knowledge of the properties of low-lying levels of ^{115}In.

ACKNOWLEDGMENTS

This work was supported in part by the US Department of Energy, Office of Nuclear Physics, under Grant No. DE-FG02-97ER41033, and performed under the auspices of the US Department of Energy by Lawrence Livermore National Laboratory under Contract No. DE-AC52-07NA27344. The authors acknowledge contributions from D. Wilmsen and U. Koester, ILL.

[1] M. Goldhaber, R. D. Hill, and L. Szilard, Phys. Rev. **55**, 47 (1939).
[2] B. Pontecorvo and A. Lazard, C.R. Acad. Sci., Paris **208**, 99 (1938).
[3] O. V. Bogdankevich, L. E. Lazareva, and F. A. Nicolaev, Zh. Eksp. Teor. Fiz. **31**, 405 (1956).
[4] J. Huizenga and R. Vandenbosch, Nuclear Physics **34**, 457 (1962).
[5] W. Varhue and T. Williamson, Int. J. Radiat. Appl. Instrum. Part A **37**, 155 (1986).
[6] L. Dzhilavyan, V. Kauts, A. Chuprikov, and V. Furman, Yad. Fiz. **51**, 336 (1990).
[7] Y. Gangrsky, A. Tonchev, and N. Balabanov, Phys. Part. Nucl. **27**, 428 (1996).
[8] P. Walker and G. Dracoulis, Nature **399**, 35 (1999).
[9] https://www.nndc.bnl.gov/.
[10] J. Law and F. A. Iddings, J. Radioanal. Chem. **3**, 53 (1969).
[11] A. Ljubičić, K. Pisk, and B. A. Logan, Phys. Rev. C **23**, 2238 (1981).
[12] P. von Neumann-Cosel, A. Richter, C. Spieler, W. Ziegler, J. Carroll, T. Sinor, D. Richmond, K. Taylor, C. Collins, and K. Heyde, Phys. Lett. B **266**, 9 (1991).
[13] D. Belic, J. Besserer, C. Arlandini, J. de Boer, J. Carroll, J. Enders, T. Hartmann, F. Käppeler, H. Kaiser, U. Kneissl, M. Loewe, H. Maser, P. Mohr, P. von Neumann-Cosel, A. Nord, H. Pitz, A. Richter, M. Schumann, S. Volz, and A. Zilges, Nucl. Instrum. Meth. A **463**, 26 (2001).
[14] W. Alston, Phys. Rev. **188**, 1837 (1969).
[15] M. Boivin, Y. Cauchois, and Y. Heno, Nucl. Phys. A **176**, 626 (1971).
[16] M. Boivin, Y. Cauchois, Y. Heno, and V. Zecevic, Nucl. Phys. A **204**, 220 (1973).
[17] Y. Cauchois, H. Abdelaziz, R. Khérouf, and C. Schloesing-Möller, J. Phys. G: Nucl. Phys. **7**, 1539 (1981).
[18] C. B. Collins, J. A. Anderson, Y. Paiss, C. D. Eberhard, R. J. Peterson, and W. L. Hodge, Phys. Rev. C **38**, 1852 (1988).
[19] E. C. Booth and J. Brownson, Nucl. Phys. A **98**, 529 (1967).
[20] M. Berger, J. Hubbell, S. Seltzer, J. Chang, J. Coursey, R. Sukumar, D. Zucker, and K. Olsen, "XCOM: Photon cross sections database," www.nist.gov/pml/xcom-photon-cross-section-database, NBSIR 87-3597.
[21] O. Bersillon, F. Gunsing, E. Bauge, R. Jacqmin, and S. Leray, eds., *TALYS-1.0* (EDP Sciences, Nice, France, 2008).
[22] http://www.talys.eu/home/.
[23] A. Koning, S. Hilaire, and S. Goriely, Nuclear Physics A **810**, 13 (2008).
[24] W. Dilg, W. Schantl, H. Vonach, and M. Uhl, Nucl. Phys. A **214**, 269 (1973).
[25] A. V. Ignatyuk, J. L. Weil, S. Raman, and S. Kahane, Phys. Rev. C **47**, 1504 (1993).
[26] S. Goriely, S. Hilaire, and A. J. Koning, Phys. Rev. C **78**, 064307 (2008).
[27] D. Brink, Nuclear Physics **4**, 215 (1957).
[28] P. Axel, Phys. Rev. **126**, 671 (1962).
[29] S. Goriely, S. Hilaire, M. Girod, and S. Péru, Phys. Rev. Lett. **102**, 242501 (2009).
[30] S. Goriely, S. Hilaire, S. Péru, and K. Sieja, Phys. Rev. C **98**, 014327 (2018).
[31] V. Varlamov, B. Ishkhanov, V. Orlin, and A. Sopov, Rept: MSU-INP **2010**, 8 (2010).